

A Quadrant-CCD star tracker

M. Clampin, S. T. Durrance, R. Barkhouser, D. A. Golimowski, A. Wald and W. G. Fastie

Centre for Astrophysical Sciences,
The Johns Hopkins University, Baltimore, MD21218.

D.L Heidtmann and M. M. Blouke

Tektronix Inc, Beaverton, OR 97077.

J. A. Westphal

Division of Geological and Planetary Sciences,
California Institute of Technology, Pasadena, CA 91125.

J.R Janesick

Jet Propulsion Laboratory,
Pasadena, CA 91125.

J.E. Gunn,

Department of Astrophysical Sciences,
Princeton University, Princeton, NJ 08544.

ABSTRACT

We discuss the characteristics of a Quadrant-CCD developed by Tektronix for pointing and tracking applications. The device is discussed in the context of its application to the Johns Hopkins University adaptive optics program, where it is being used for the correction of stellar image motion resulting from atmospheric turbulence. The transfer function of the device is discussed and results are presented which demonstrate the Quadrant-CCDs capability to provide offset signals to control a rapid guiding mirror in the Johns Hopkins instrument.

1. INTRODUCTION

The Johns Hopkins University (JHU) has recently started a program to develop adaptive optics with the purpose of studying, at high spatial resolution, the distribution of circumstellar material around bright stars, such as β Pictoris¹, in the optical and near-IR. Adaptive optics has the potential to permit ground-based telescopes to reach near-diffraction limited imaging by correcting in real time for the effects of atmospheric turbulence known as "seeing". The JHU program is evolutionary in its approach, with the correction for the wavefront tilt (image motion) component of seeing being implemented initially, to be followed by a fully adaptive system based on a membrane mirror at a later stage.

The image motion compensation system consists of a sensor which measures the image offset at 10-200 ms intervals and converts the offset to a series of three voltages which are input to a high speed tip/tilt mirror. For the first phase of the program, a sensor capable of rapidly detecting the motion of a point source was required. Since the frequency spectrum of image motion contains significant power out to ~ 50

Hz for smaller aperture telescopes (0.5 - 1.5 meter diameter), closed loop correction rates up to ~ 300 Hz are required. We selected the Quadrant-CCD which had been built by Tektronix in collaboration with J. Westphal as part of an earlier investigation of alternative fine guidance sensors for the Hubble Space Telescope led by W. G. Fastie² at Johns Hopkins University. In this paper we discuss the characteristics of the Quadrant-CCD and present some laboratory results demonstrating its performance as an image motion sensor in the JHU adaptive optics system.

2. QUADRANT-CCD DESIGN AND CONTROL

The Quadrant-CCD is a 3-phase, frontside illuminated device. As its name implies the parallel register of the CCD comprises four $100\text{ }\mu\text{m}$ square pixels, which are read out through a single serial register. During operation, the point source target is imaged onto the center of the CCD and when the CCD is read out, it produces four intensity values which allow the determination of an offset from the null position corresponding to the location of the image during integration. The architecture of the Quadrant-CCD is shown in figure 1. Since the four pixels are read out through a single serial register it is necessary that the quadrant architecture is divided in one direction by a channel stop and in the opposite direction by a gate electrode $\phi 1$.

It is desirable to reduce the dark noise of the CCD even for short exposure times of 10 - 200 milliseconds, in order to maximize the dynamic range of the device and to reduce signal processing during calculation of the offset positions. The Quadrant-CCD is typically cooled to temperatures of -35 to -40°C which gives negligible dark noise for short exposures. We have chosen to cool the devices using 3 or 4 stage thermoelectric (Peltier) stacks which are compact and easy to operate. The Quadrant-CCD is housed in an evacuated lightweight aluminium dewar. A small fluid bath in the base of the dewar is fed by a closed circuit chiller and removes heat from the hot face of the thermoelectric cooler. The Quadrant-CCD package is mounted on a circular circuit board containing the clock and preamplifier circuitry and is thermally coupled to the thermoelectric stack by a short copper finger.

The controller electronics for the Quadrant-CCD are a modified version of the Palomar Observatory system described in detail by Gunn et al³. While the circular board containing clock drivers and preamplifier has been redesigned for the Quadrant-CCD, the remaining components of the system are essentially unchanged and consist of logic, bias, Analogue-Digital and signal chain circuit boards together with their respective power supplies. These units are packaged in two small boxes which mount on the instrument close to the Quadrant-CCD.

A PC-based data acquisition computer controls the CCD system via a DMA card which interfaces to the CCD controller. In addition to reading the Quadrant-CCD pixel values, the PC also controls the closed feedback loop which operates the tip/tilt mirror. Data reads are initiated by sending a linestart signal to the CCD controller. Since it takes 1.2 ms to read the chip, compute the position error signals and output the corrections to the tip/tilt mirror, CCD integration times of at least 2 ms are needed for operation of the feedback loop. During the computation of position errors, the events are thresholded to discriminate cosmic ray events and if the image position offset exceeds a predefined value the imaging camera's shutter is closed. This allows short periods of bad seeing to be rejected in real time, thus improving the quality of the final image. There is a relatively short time lag between measurement of the position offset and application of the tip/tilt mirror correction making the system less susceptible to feedback instabilities.

For a 1 metre telescope typical integration times of 10-20 ms are required to adequately sample the image motion power spectrum. The system software provides interactive display of the Quadrant-CCD error signal simplifying the process of aligning and focusing elements within the instrument. During operation of the image motion compensation feedback loop, a real time display provides a plot of the error signal together with data relating to the image motion statistics. Segments of image motion data may also be written to disk for subsequent frequency spectrum analysis.

3. QUADRANT-CCD CHARACTERISTICS

The full well of the Quadrant-CCD is $\sim 500,000 e^-$ and is adequate for our application. Read out noise levels as low as $\sim 10 e^-$ has been achieved with the devices we have tested, an important consideration, since flux levels from stellar point sources, given 10-200 ms exposures, are relatively low. The peak quantum efficiency of the device is $\sim 50\%$ at 600 nm with spectral response extending from $\sim 450 - 1000$ nm. The poor blue response below 400 nm is not important for our application since we are primarily interested in imaging in the bandpass 500-900 nm. The uniformity of the device is difficult to accurately quantify given its small format, however, for the devices we have evaluated the pixel to pixel non-uniformity has ranged between 2%-10 %.

The performance of the Quadrant-CCD as an image motion sensor is determined by the transfer function in the X and Y directions, given by

$$T_X = (Q_1 + Q_2 - Q_3 - Q_4) / \Sigma Q_N$$

$$T_Y = (Q_1 + Q_4 - Q_2 - Q_3) / \Sigma Q_N$$

respectively, where Q_N is the signal from pixel N in the Quadrant-CCD. In figure 2 we show two typical transfer curves for the X and Y directions along the chip measured with a $10 \mu\text{m}$ pinhole image. The two transfer functions show reciprocal gradients of 17 and $13 \mu\text{m}$ respectively. The slight disparity between the two curves is a result of the electrode architecture of the Quadrant-CCD. The parallel register is divided by a channel stop in the X direction and a gate electrode ($\phi 1$) in the Y direction, which both obscure light. The attenuation of light by these electrodes is illustrated by the sum-signal curves which overlay the transfer functions in figure 2. The difference in transfer function gradient is not large enough to have a significant effect upon the performance of the JHU image motion compensation system. During operation of the image motion compensation system this disparity is corrected by using two different gain factors in calculating the tip/tilt mirror offset.

4. RESULTS

In figure 3 we show the results of a laboratory simulation to evaluate the performance of the Quadrant-CCD operating as an image motion sensor. These experiments were performed using the image of a pinhole where simulated random image motion, having frequency characteristics comparable with a good astronomical site⁴, is generated using a second tip/tilt mirror. The first two images show a profile and contour map of an image with simulated image motion giving an image of $\sim 1''$ FWHM. The second two images show the profile and contour map obtained with the image motion compensation loop operational, the simulated stellar profile is essentially diffraction limited. The simulation does not take account of the effects of phase distortion in real stellar images, but clearly demonstrates the effectiveness of the Quadrant-CCD in tracking the image by providing accurate offsets to control the tip/tilt mirror. Field testing of the system on astronomical telescopes has recently commenced.

The suitability of the Quadrant-CCD as a fine guidance sensor for Space Telescope has been reviewed by Fastie². A related study by D. Schroeder² analytically confirms that a system based on a Quadrant-CCD may be used to point a Space Telescope and also monitor the diffraction limited image. These theoretical studies together with our experimental evaluation of the Quadrant-CCD demonstrate the suitability of the Quadrant-CCD for space-based pointing and tracking applications.

5. FUTURE DEVELOPMENTS

A second generation of Quadrant-CCDs has recently been fabricated by Tektronix which offer improved performance in terms of readout time, read noise and transfer function uniformity as a result of changing the architecture of the CCD. In the new design four separate serial registers, one for each pixel, allow each pixel to be individually read. This permits a modified electrode structure eliminating the slight difference in transfer functions resulting from the presence of the channel stop. The CCD readout the readout time is also decreased, allowing integration times of the order of μs . Even though the existing Quadrant-CCD design is fast enough for our application, the new device will permit us to reduce the time between the CCD read and the output of tip/tilt mirror control voltages still further. A further reduction in read noise below the current level of $\sim 10\text{ e}^-$ will also be obtained as a result of the new design. We expect to start tests of these new devices in the near future.

In future designs thinning of the CCD should be considered, since this would permit operation as backside illuminated devices yielding improved quantum efficiencies. Backside illumination would also improve the gradient of the transfer function since there are no obscurations due to the device's electrode structure. Experience with the Quadrant-CCD suggests that increasing the number of pixels to a 4×4 array of $50\text{ }\mu\text{m}$ square pixels would allow detailed diagnostics of the point source, especially useful for focussing. Operation as a quadrant device would still be possible by binning the pixels as the CCD is read out. For wavefront sensing applications arrays of Quadrant-CCDs are an obvious possibility for high speed Shack-Hartmann wavefront sensors.

6. ACKNOWLEDGEMENTS

The Johns Hopkins University wishes to thank the Seaver Institute for their generous support of the Johns Hopkins adaptive optics program.

7. REFERENCES

1. Smith, B. and Terrile, R., 1984, *Science*, **226**, 1421.
2. Fastie, W. G., 1989, Study of Fine Guidance Systems for the Hubble Space Telescope, Final Report NASA Contract NAS8-35348.
3. Gunn, J. E., Emory, E. B., Harris, F. H. and Oke, J. B., 1987, *P.A.S.P.* **99**, 518.
4. Martin, H. M., 1987, *P.A.S.P.* **99**, 1360.

Figure 1 : Schematic showing the architecture of the Quadrant-CCD.

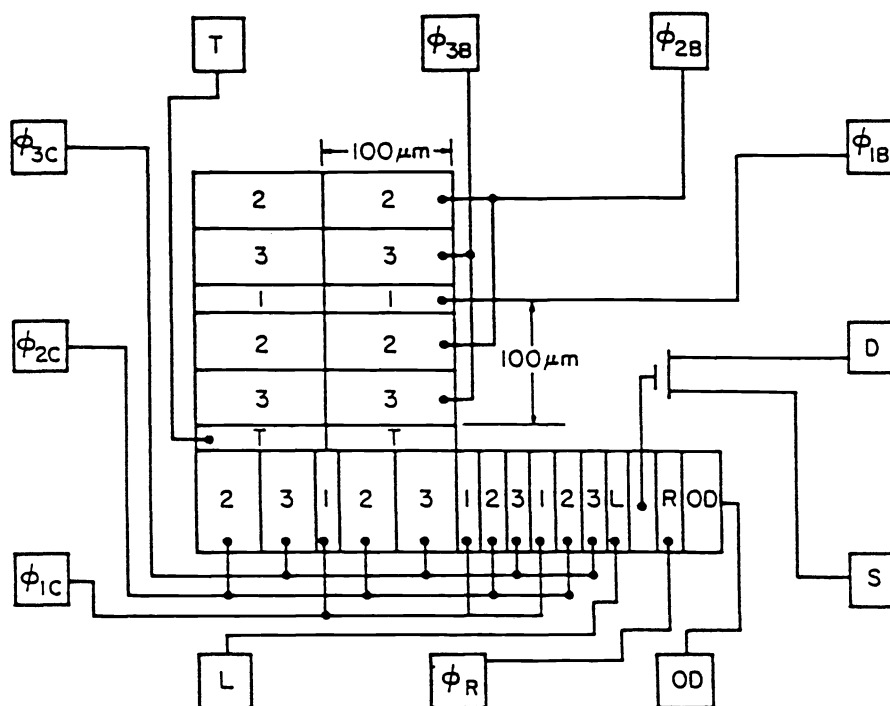
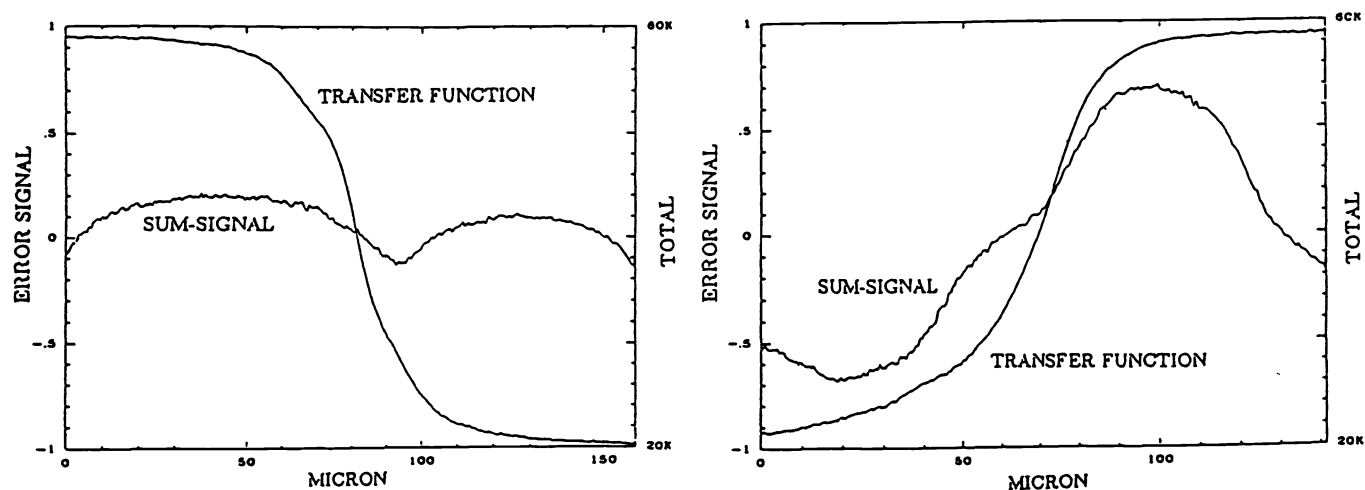


Figure 2 : Transfer curves and summed signal plots obtained by scanning a 10 μm pinhole image across the Quadrant-CCD horizontally (right) and vertically (left) axes.



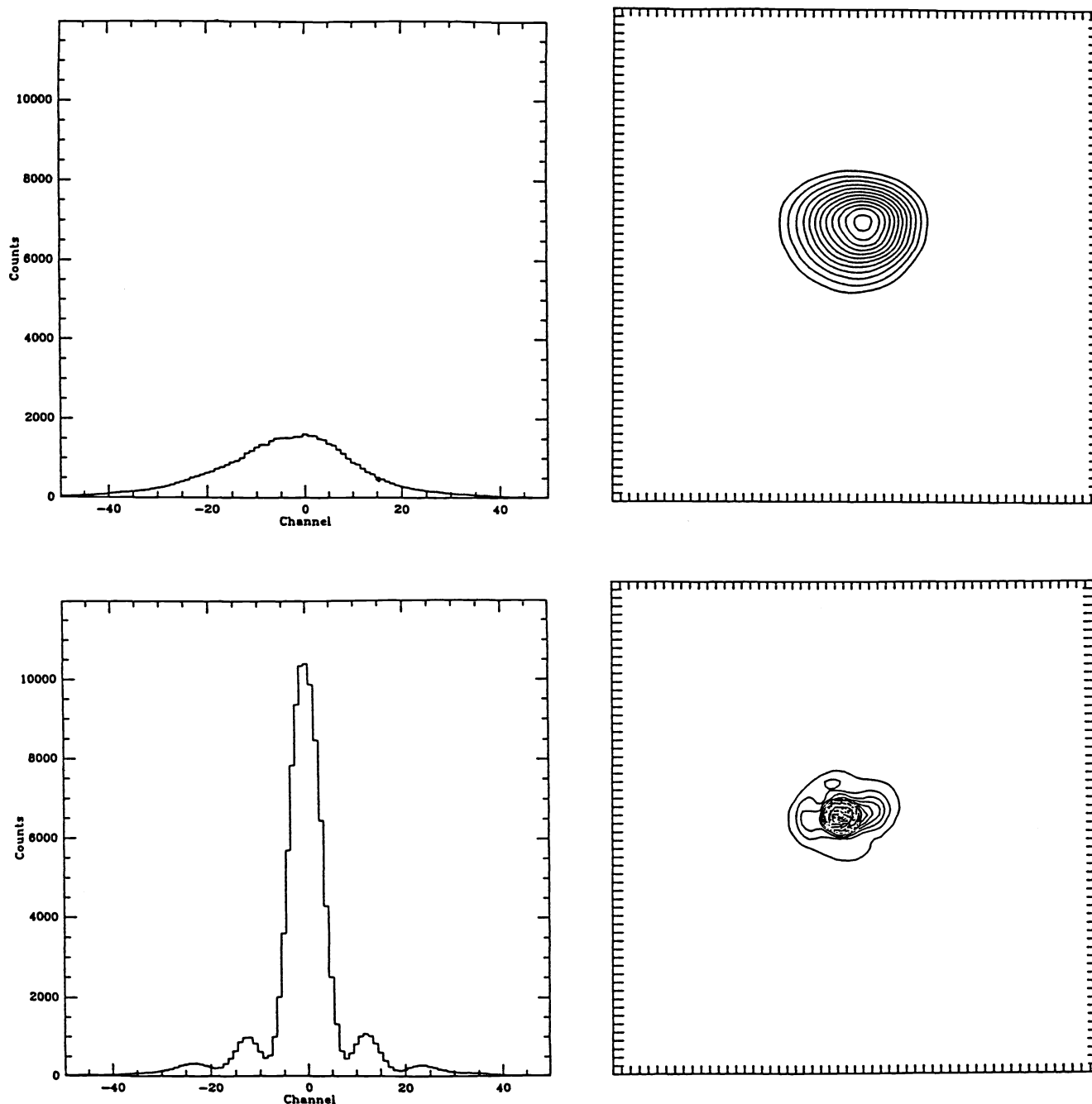


Figure 3 : A laboratory simulation demonstrating the use of a Quadrant-CCD in correcting for the effects of atmospheric distortion on stellar images. The upper profile and contour plot show a pinhole degraded by random image motion having appropriate frequency spectrum⁴. The lower two plots demonstrate the improved pinhole image obtained with the image motion compensation loop operational and a Quadrant-CCD integration time of 10 ms.